

AN EVALUATION OF THE OPTICAL MASER PHOTON RATE GYROSCOPE

C. V. Heer

Department of Physics, Ohio State University, Columbus, Ohio

UNPUBLISHED PRELIMINARY DATA

Paper Presented at
Colloque Sur Les Gyroscopes Avances
2-6 November 1964

Sponsored by
Centre National D'Etudes Spatiales
Paris, France

FACILITY FORM 802	N66 33411	
	(ACCESSION NUMBER)	(THRU)
	39	/
	(PAGES)	(CODE)
	CR-59809	16
	(NASA CR OR TMX OR AD NUMBER)	(CATEGORY)

Research Investigation Supported in part by NASA Grant
No. NsG-552

GPO PRICE \$ _____

CFSTI PRICE(S) \$ _____

Hard copy (HC) 2.00

Microfiche (MF) .50

An Evaluation of the Optical Maser Photon
Rate Gyroscope*

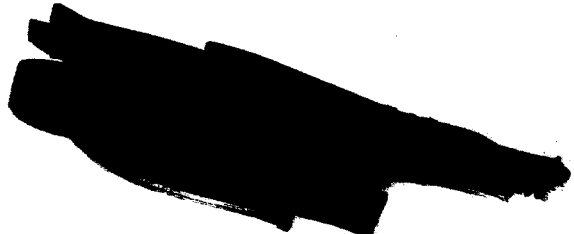
C.V. Heer

Department of Physics, Ohio State University, Columbus, Ohio

INTRODUCTION

N66 53411

The measurement of absolute rotation with electromagnetic radiation was suggested by Michelson¹ in 1904 on the basis of the "ether". Observations of subsequent investigators² confirmed the measurement of rotation by using an interference technique, and in 1925 Michelson and Gale³ succeeded in measuring the angular rotation of the earth with an optical system approximately one kilometer in diameter. With the advent of general relativity it was shown that problems related to the transmission of electromagnetic radiation in accelerated frames of reference were more properly treated within the framework of general relativity. Adopting this viewpoint the author pointed out in 1961 that the degeneracy between clockwise and counter-clockwise traveling waves in a resonant electromagnetic structure is removed by rotation and an angular frequency difference between the two modes of $2m\Omega$ would occur in a cylindrical cavity⁴. The name "Coriolis-Zeeman" effect for a photon was suggested during the presentation of the paper, since for an electromagnetic cavity with cylindrical symmetry or other suitable shapes, the energy transformation for a photon is given by $h\nu \approx h\nu_0 + \underline{L} \cdot \underline{\Omega}$. \underline{L} is the orbital angular



momentum of the photon about the symmetry axis and Ω is the angular velocity of the cavity. If m is the number of nodes, $L_z = m\hbar$ and $\Delta\omega = 2m\Omega$.

In subsequent papers a formal development for the resonant frequencies of an electromagnetic cavity in an accelerated frame of reference was given.^{5,6} The results of these papers are summarized for this paper. If a system rotates with angular velocity $\underline{\Omega} = \Omega \hat{a}_z$ about the z-axis, for cartesian ordering of the coordinates Maxwell's equations have their conventional appearance in the m.k.s. system of units,

$$\begin{aligned} \text{curl } \underline{E} + \frac{\partial \underline{B}}{\partial t} &= 0 & \text{div } \underline{B} &= 0 \\ \text{curl } \underline{H} - \frac{\partial \underline{D}}{\partial t} &= \underline{J} & \text{div } \underline{D} &= \rho \end{aligned} \quad (1)$$

The constitutive equations are modified by rotation and are given to first order in Ω by

$$\underline{B} = K_m \mu_0 \underline{H} + c^{-1} \left[\left(\frac{\underline{\Omega} \times \underline{r}}{c} \right) \times \underline{E} \right] + \mathcal{O}(\Omega^2) \quad (2a)$$

$$\underline{D} = K_e \epsilon_0 \underline{E} - c^{-1} \left[\left(\frac{\underline{\Omega} \times \underline{r}}{c} \right) \times \underline{H} \right] + \mathcal{O}(\Omega^2) \quad (2b)$$

In the short wave length limit these equations are equivalent to an index of refraction

$$\mu = (K_e K_m)^{\frac{1}{2}} + c^{-1} (\underline{\Omega} \times \underline{r}) \cdot \hat{K}_0 + \mathcal{O}(\Omega^2) \quad (3)$$

where \hat{K}_0 is a unit vector in the direction of propagation. Rotation has the effect of making even the vacuum appear anisotropic. Equations

2a and 2b are the constitutive equations relating the fields. The current \underline{J} is the source or detector term and is associated with the source and detector attached to the cavity, that is the electromagnetic cavity, source, and detector are all in the same rotating frame of reference. The explicit dependence of \underline{J} on the magnetic dipole currents and electric dipoles may be shown by writing \underline{J} as $\underline{J} + \text{curl } \underline{M} + \partial \underline{P} / \partial t$. If the source or detector current is of the ohmic type and proportional to the electric field, that is σE or $\epsilon'' E$, then the correction due to rotation is of $O(\Omega^2)$. Thus the source and detector terms have their conventional form for the first order approximations used in this paper. If the fields are expanded in a set of orthonormal functions \underline{E}_a and \underline{H}_a for $\Omega = 0$, the frequency splitting between the degenerate modes which is introduced by rotation is

$$\frac{\Delta \nu}{\nu_a} = (K_e K_m c^{-2})^{-\frac{1}{2}} \underline{\Omega} \cdot \int dv \left[\underline{r} \times (\underline{E}_a \times \underline{H}_a^* + \underline{E}_a^* \times \underline{H}_a) \right] + O(\Omega^2) \quad (4)$$

Although our initial interest was in the microwave cavities and the enhancement of the Q of these cavities with maser media⁷, the advent of optical masers provided an enhanced sensitivity and a Fabry-Perot square resonator with an optical maser medium to provide oscillations at both clockwise and counter-clockwise frequencies and with an output beat frequency proportional the angular rotation was proposed⁹. Such beats due to rotation were first reported by Mack and Davis¹⁰, and subsequently by Cheo¹¹, and by many other investigators. Some schematic diagrams of

optical resonant cavities are shown in Figure 1. These are closed path Fabry-Perot structures with all flat or with one or more curved mirrors. Fox and Li¹¹ have shown that structures with diffraction losses possess normal modes. Equations for the resonators shown in Figure 1 have been developed by Collin's and by other investigators¹². These almost plane wave expansions may be used with equation 4 to determine the beat frequency.

EQUATIONS OF MOTION OF THE CAVITY MODES

The quasi-modes developed for the cavities with diffraction losses shown in Figure 1 cannot be expressed in simple analytic form over the cavity. Fox and Li have shown that there is a similarity between TE waveguide modes and the TEM modes which occur in these partially open structures. In order to simplify the calculations it is convenient to use a waveguide bent into a circle as shown in Figure 2 and for which a simple approximate normal mode expansion exists. A cavity with lossless walls could be regarded as the ideal cavity for the photon rate gyroscope. The normal mode expansion of a waveguide bent into a circle of large radius R is approximately given by

$$\underline{E}_{mnq} \approx \underline{u}_{mn} \frac{e^{iqf}}{(2\pi)^{1/2}} = \underline{u}_{mn} U_q \quad ; \quad \underline{H}_{mnq} \approx (iq/cR) (\hat{a}_\varphi \times \underline{E}_{mnq})$$

$$\omega_{mnq}^2/c^2 = k_{mn}^2 + (q/R)^2 \quad (6)$$

\underline{u}_{mn} is the transverse mode of the guide and is given by the solution of the boundary value problem for the guide cross-section. \underline{u}_{mn} may be derived

from a scalar wavefunction ψ_{mn} where ψ_{mn} is a solution of

$$\nabla^2 \psi_{mn} + k_{mn}^2 \psi_{mn} = 0 \quad u_{mn} = -\left(\hat{a}_\varphi \times \text{grad } \psi_{mn}\right) \rho_{mn}^{-1}$$

For the TE modes of a rectangular wave guide ψ_{mn} is given by

$$\psi_{mn} = 2(L_x L_y)^{-\frac{1}{2}} \cos\left(\frac{m\pi x}{L_x}\right) \cos\left(\frac{n\pi y}{L_y}\right); \quad k_{mn}^2 = (m\pi/L_x)^2 + (n\pi/L_y)^2$$

q is an integer of the order of 10^6 , R the order of a meter, m and n integers of the order of unity, and L_x and L_y the order of millimeters.

ψ_{mn} may be determined for other cross-sections. The cross-sections for the open structures shown in Figure 1 can be approximated by using simple harmonic oscillator wavefunctions for the transverse mode and this implies that the transverse equation is of the form $\nabla^2 \psi_{mn} + (k_x^2 x^2 + k_y^2 y^2) \psi_{mn} = 0$. A proper choice of k_x^2 and k_y^2 based on the curvature of the mirrors and the distance between the mirrors yields an expression for the oscillation frequency in good agreement with the integral equation development. This similarity appears since the solution of the simple harmonic oscillator equation yields $(m + \frac{1}{2})$ and $(n + \frac{1}{2})$ corrections to the resonant frequency of the oscillator.

Using the three index notation for a normal mode the general equations given by Heer^{5,6} for the time dependent coefficients may be written as

$$\begin{aligned} \int \underline{E} \cdot \underline{E}_a^* &= E'_{mnq}; & \int \underline{H} \cdot \underline{H}_a^* &= H'_{mnq}; & \int \underline{J} \cdot \underline{E}_a^* &= P'_{mnq} \\ \int \underline{B} \cdot \underline{H}_a^* &= K_m \mu_0 H'_{mnq} - \frac{\Omega R}{c} E'_{mnq}; & \int \underline{D} \cdot \underline{E}_a^* &= K_e \epsilon_0 E'_{mnq} - \frac{\Omega R}{c} H'_{mnq} \end{aligned} \quad (7)$$

For small Ω the equation of motion for the time dependent coefficient of motion for the time dependent coefficient of the normal mode E_{mnq} is given by

$$\ddot{E}_{mnq} + \omega_{mnq}^2 E_{mnq} - i2\Omega q \dot{E}_{mnq} = -\epsilon_0^{-1} \ddot{P}_{mnq} - \frac{\omega_{mnq}}{Q_{mnq}} \dot{E}_{mnq} \quad (8)$$

The terms on the left are for a lossless cavity undergoing rotation about the z-axis at angular velocity Ω . On the right hand side the first term is the macroscopic polarization or source term and the second term includes the cavity losses and other loads. If Q_{mnq} is chosen as a function of frequency and complex, the frequency pulling by a load as well as load losses may included in this single term. In the absence of a source or loss term the resonant frequency of the cavity is given by

$$\omega^2 - \omega_{mnq}^2 + 2\Omega q \omega = 0$$

or to first order by

$$\omega_{mnq} \approx \pm \omega_{mnq}^0 - \Omega q \quad (9)$$

This is in accord with the earlier expression for the frequency difference between clockwise traveling waves, positive q , and counter-clockwise traveling waves, negative q ,

$$\Delta \nu_q \approx (2\Omega q / 2\pi) = 2R\Omega / \lambda_q \quad (10)$$

If the cavity axis and the axis of rotation are not parallel then the beat frequency should be obtained using equation 4. For simple structures

with an angle γ between the two axes, equation 10 is multiplied by $\cos \gamma$.

Only the q or peripheral dependence of the mode is effected by rotation. Regarding this as a first order effect, the transverse waves are effected in second or higher orders by rotation.

Single Mode Excitation

The general case is much too complex for ready analysis and the excitation of the cavity in an almost degenerate single clockwise and counter-clockwise mode is considered. This is the simplest and most important case. If the losses of the system are small or the Q is sufficiently large that the frequency separation between modes is large compared to the bandwidth of the cavity, it is always possible to tune the cavity for oscillation at a single mode. If this mode is denoted as q with linear polarization, then

$$E_{mnq} \rightarrow (2\pi)^{-\frac{1}{2}} \underline{u} e^{\pm iq\varphi} \quad (11)$$

where \underline{u} is the linear polarization of the transverse mode and q is a positive number. The electric field in the cavity is given by

$$\underline{E}(\underline{r}, t) = E_{+q}(t) \underline{u} \frac{e^{+iq\varphi}}{(2\pi)^{\frac{1}{2}}} + E_{-q}(t) \underline{u} \frac{e^{-iq\varphi}}{(2\pi)^{\frac{1}{2}}} \quad (12)$$

where in accordance with the earlier development

$$E_{+q}(t) = \int dv \underline{E} \cdot \left((2\pi)^{-\frac{1}{2}} \underline{u} e^{iq\varphi} \right)^* \quad (13a)$$

According to equation 8 the source for mode (mq) or for $E_{+q}(t)$ is $P_{+q}(t)$, where $P_{+q}(t)$ is given by

$$P_{+q}(t) = \int dv \underline{P} \cdot \left((2\pi)^{-\frac{1}{2}} \underline{u} e^{iq\varphi} \right)^* \quad (13b)$$

The fields and polarization are real vectors and this requires

$$E_{-q}(t) = E_{+q}^*(t) \quad ; \quad P_{-q}(t) = P_{+q}^*(t) \quad (13c)$$

Using equation 8, the equation of motion for this single may be re-written as

$$\ddot{E}_{+q} + \omega_0^2 E_{+q} - i2\Omega q \dot{E}_{+q} = -\epsilon_0^{-1} \ddot{P}_{+q} - \frac{\omega_0}{Q} \dot{E}_{+q} \quad (14)$$

where ω_0 is the resonant frequency of the non-rotating lossless cavity.

The time dependence of the field in a cavity without losses or sources, that is the right hand side of equation 14 is zero, is

$$E_{+q}(t) = A' e^{-i(\omega_0 - \Omega q)t} + B' e^{+i(\omega_0 + \Omega q)t} \quad (15a)$$

The term with the A coefficient corresponds to the counter-clockwise traveling wave and the term with the B coefficient to the clockwise traveling wave. This notation will be used in the remainder of the paper. Since ω_0 is large compared to the other effects, equation 14 will be examined for fields

$$E_{+q}(t) = A(t)e^{-i\omega_0 t} + B(t)e^{+i\omega_0 t} \quad (15b)$$

where $A(t)$ and $B(t)$ are slowly varying functions of time. Further reduction requires an expression for $P_{+q}(t)$ in terms of the electric field $E_{+q}(t)$.

This is not the most general development for single mode operation. Linear polarization is used. If the canonical states of polarization u_{\perp} and u_{\perp}^* are used, then four terms are needed in equation 12. The space modes are $u_{\perp} e^{\pm iq\varphi}$ and $u_{\perp}^* e^{\pm iq\varphi}$.

POLARIZATION OF THE OPTICAL MASER MEDIUM

The polarization of the optical maser medium is investigated using a procedure similar to that introduced by Lamb.¹³ For convenience it is assumed that the dominant interaction of a perturbing field with an atom is between two energy levels a and b as shown in Figure 3. If the hamiltonian of the interaction is of the form $H = H_0 + H_1(t)$ with a time dependent matrix element

$$\mathcal{H}V(t) = (a|H_1|b) = (b|H_1|a)^* \quad (16)$$

the phenomenological equations of motion for the bilinear form of an atom are given by,

$$\dot{\rho}_{ab} = (-\gamma_{ab} - i\omega_{ab})\rho_{ab} + iV(\rho_{aa} - \rho_{bb}) \quad (17)$$

$$\dot{\rho}_{ba} = \dot{\rho}_{ab}^*$$

$$\dot{\rho}_{aa} = -\gamma_a \rho_{aa} + i[V^* \rho_{ab} - \rho_{ba} V] + \lambda_a$$

$$\dot{\rho}_{bb} = -\gamma_b \rho_{bb} - i[V^* \rho_{ab} - \rho_{ba} V] + \lambda_b$$

The γ 's and λ 's are introduced in a phenomenological manner to correspond to excitation and damping. This set of differential equations may be placed in integral form by noting that the general solution to the equation

$$\dot{x} = -\gamma x + f(t) + \lambda$$

is
$$x(t) = \left[x(t_0) - \lambda/\gamma \right] e^{-\gamma(t-t_0)} + \lambda/\gamma + \int_{t_0}^t dt' e^{-\gamma(t-t')} f(t')$$

Since only the steady state solution is of interest, t_0 is chosen at $-\infty$ and the quantities of physical interest are described by the integral equation,

$$x(t) = \lambda/\gamma + \int_0^{\infty} ds e^{-\gamma s} f(t-s) \quad (18)$$

The physical observables of interest are described by the integral form of the density matrix,

$$\begin{aligned} \rho_{ab}(t) &= i \int_0^{\infty} ds' \exp -(\gamma_{ab} + i\omega_{ab})s' V(t-s') [\rho_{aa}(t-s') - \rho_{bb}(t-s')] \\ \rho_{aa}'(t) &= \lambda_a/\gamma_a + i \int_0^{\infty} ds' e^{-\gamma_a s'} [V^*(t-s') \rho_{ab}(t-s') - \rho_{ba}(t-s') V(t-s') + \lambda_{1a}(t-s')] \end{aligned} \quad (19)$$

etc.

λ_1 contains the time dependent part of λ and this is neglected in the following. The experimental quantity of interest is ρ_{ab} and direct substitution yields

$$\begin{aligned} \rho_{ab}(t) &= i \int_0^{\infty} ds' \exp -(\gamma_{ab} + i\omega_{ab})s' V(t-s') \left\{ (\lambda_a/\gamma_a - \lambda_b/\gamma_b) \right. \\ &\quad \left. + \int_0^{\infty} ds'' (e^{-\gamma_a s''} + e^{-\gamma_b s''}) (iV^*(t-s'-s'') \rho_{ab}(t-s'-s'') + c.c.) \right\} \\ &= \rho_{ab}^{(1)}(t) + \rho_{ab}^{(3)}(t) + \dots \end{aligned} \quad (20)$$

An interaction solution yields the following first order and third order terms

$$\rho_{ab}^{(1)}(t) = i(\lambda_a/\gamma_a - \lambda_b/\gamma_b) \int_0^\infty ds' [\exp -(\gamma_{ab} + i\omega_{ab})s'] V(t-s') \quad (21a)$$

$$\rho_{ab}^{(3)}(t) = -i(\lambda_a/\gamma_a - \lambda_b/\gamma_b) \int_0^\infty ds' ds'' ds''' [\exp -(\gamma_{ab} + i\omega_{ab})s'] V(t-s') \\ (e^{-\gamma_a s''} + e^{-\gamma_b s''}) \left\{ [\exp -(\gamma_{ab} + i\omega_{ab})s'''] V^*(t-s'-s'') V(t-s'-s''-s''') + c.c. \right\} \quad (21b)$$

Doppler Effect

$\rho_{ab}(t)$ is determined by the perturbation $V(t)$ as seen by the atom. Since equations for the classical fields and polarization are referred to a frame of reference attached to the cavity, it is desirable to have $\rho_{ab}(\underline{r}, t)$ in the same reference frame. If an atom enters state "a" at time t_e at position \underline{r}_e with velocity \underline{v} , it contributes to $\rho(\underline{r}, t; \underline{v})$ if

$$\underline{r}_e = \underline{r} - \underline{v}(t-t_e)$$

The perturbation experienced by the atom with an electric dipole moment

ρ_{ab} is of the form

$$V(t') = -\frac{1}{\hbar} \underline{\mu}_{ab} \cdot \underline{E}_{atom}(t') \quad (22)$$

where $\underline{E}(t')$ is the field determined by the moving atom. If $\underline{E}(\underline{r}, t)$ is the cavity field at position \underline{r} at time t , then

$$\underline{E}(t') = \underline{E}(\underline{r}_e + \underline{v}(t'-t_e), t') = \underline{E}(\underline{r} - \underline{v}(t-t'), t') \quad (23)$$

is the relationship between the electric field at the atom and the cavity electric field \underline{E} . Equation 21a and 21b for $\rho_{ab}(t)$ give $\rho_{ab}(\underline{r}, t; \underline{v})$

when $V(t-s) \longrightarrow V(\underline{r}-\underline{v}s; t-s)$ (24a)

$$\rho_{ab}(t) \longrightarrow \rho_{ab}(\underline{r}, t; \underline{v}) \quad (24b)$$

Only the component of the velocity in the direction of the traveling wave is important for the doppler effect. In the circular cavity, $\underline{v} = R \dot{\phi} \hat{u}_{\phi}$. The velocity distribution is given by the one-dimensional Maxwell-Boltzman distribution,

$$W(\underline{v})d\underline{v} \longrightarrow W(\dot{\phi})d\dot{\phi} = \left(\frac{m}{2\pi kT}\right)^{\frac{1}{2}} \exp - \frac{mR^2 \dot{\phi}^2}{2kT} R d\dot{\phi} \quad (25)$$

For subsequent calculations the average of $\exp(\pm iq\dot{\phi}s)$ over the velocity distribution is needed. This is given by

$$\int_{-\infty}^{\infty} d\dot{\phi} W(\dot{\phi}) \exp(\pm iq\dot{\phi}s) = e^{-1/4 D^2 s^2} \quad (26a)$$

where $D^2 = \frac{2q^2 kT}{mR^2} = \frac{8\pi^2 kT}{m\lambda^2} = \frac{\pi^2 \Delta \mathcal{V}_D^2}{\ln 2}$ (26b)

and m is the mass and λ the wavelength of the radiation.

Polarization

The macroscopic polarization $\underline{P}(\underline{r}, t)$ is a statistical average over the atoms in the vicinity of position \underline{r} at time t . Lamb¹³ has given a detailed expression for the polarization. In this paper λ is assumed constant, the number of atoms per cubic meter or N is assumed constant, and the distribution of velocities is given by equation 25. With these assumptions the polarization of a medium with atoms with two energy levels a and b and with an electric dipole moment matrix element

$$\mu_{ba} = (b|e_{\underline{r}}|a) = \mu_{ab}^* \quad (27)$$

is given by

$$P_{\underline{r}}(\underline{r}, t) \simeq N \int d\underline{v} W(\underline{v}) \left[\rho_{ab}(\underline{r}, t; \underline{v}) \mu_{ba} + \text{c.c.} \right] \quad (28)$$

This can be evaluated by direct substitution of 24a into 21a and 21b to obtain $\rho_{ab}(\underline{r}, t; \underline{v})$ to third order. The remaining terms are given by equation 25 and 27. These will be discussed for important simple examples.

First Order Polarization for Single Mode Operation

Using the previous results the first order contribution to the polarization is

$$P_{+q}^{(1)} = - \frac{N \mu_{ab}^{-1}}{2\pi} (\lambda_a / \gamma_a - \lambda_b / \gamma_b) \int dA d\underline{v} \underline{u} e^{-iq\varphi} \left\{ \int_0^\infty d\dot{\varphi} W(\dot{\varphi}) \left[i \mu_{ba} \int_c^\infty ds \exp -(\gamma_{ab} + i\omega_{ab})s \left[(\mu_{ba}^* \cdot \underline{u}) E_{+q}(t-s) \exp +i(q\varphi - q\dot{\varphi}s) \right. \right. \right. \right. \\ \left. \left. \left. + (\mu_{ba}^* \cdot \underline{u}) E_{+q}^*(t-s) \exp -i(q\varphi - q\dot{\varphi}s) \right] + \text{c.c.} \right] \right\} \quad (29)$$

This equation may be reduced by the following sequence of operations:

(a) Integrate over φ and use the orthogonality of $\exp \pm iq\varphi$ to reduce the number of terms; (b) Integrate over $\dot{\varphi}$ and use equation 26a to introduce the term $\exp(-1/4 D^2 s^2)$ into the integrand; (c) Write $E_{+q}(t-s)$ in the form introduced in equation 15b, integrate over s and omit all non-resonant terms. Then the polarization may be written as

$$P_{+q}^{(1)}(t) = - N \chi^{-1} (\lambda_a / \gamma_a - \lambda_b / \gamma_b) \alpha D^{-1} \left[Z A e^{-i \omega_0 t} + Z^* B e^{+i \omega_0 t} \right] \quad (30)$$

where Z is an abbreviation for the well known function used in the theory of doppler broadening¹⁴

$$Z(\omega_0 - \omega_{ab}, \gamma_{ab}, D) = iD \int_0^\infty ds \exp \left(i(\omega_0 - \omega_{ab})s - \gamma_{ab}s - 1/4 D^2 s^2 \right) \quad (31)$$

α is the coefficient

$$\alpha = \int dA \left| \underline{u} \cdot \underline{\mu}_{ba} \right|^2 \quad (32)$$

Third Order Polarization for Single Mode Operation

$$P_{+q}^{(3)} = \frac{N \chi^{-3} (\lambda_a / \gamma_a - \lambda_b / \gamma_b)}{(2\pi)^2} \int dA d\varphi \underline{u} e^{-i q \varphi} \int_{-\infty}^{\infty} d\psi W(\psi) \cdot \left\{ i \underline{\mu}_{ba} \int_0^\infty ds' ds'' ds''' (e^{-\gamma_a s''} + e^{-\gamma_b s''}) \right. \\ \left. \exp(-(\gamma_{ab} + i \omega_{ab})s) \left[\frac{\underline{\mu}_{ba}^* \cdot \underline{u}}{\mu_{ba}^*} E_{+q}(t-s') \exp i(q\varphi - q\psi s') + \frac{\underline{\mu}_{ba}^* \cdot \underline{u}}{\mu_{ba}^*} E_{+q}^*(t-s') \exp -i(q\varphi - q\psi s') \right] \right. \\ \left. \left[\exp(-(\gamma_{ab} + i \omega_{ab})s'' \left(\frac{\underline{\mu}_{ba}^* \cdot \underline{u}}{\mu_{ba}^*} E_{+q}^*(t-s'-s'') \exp -i(q\varphi - q\psi(s'+s'')) + \frac{\underline{\mu}_{ba}^* \cdot \underline{u}}{\mu_{ba}^*} E_{+q}(t-s'-s'') \exp i(q\varphi - q\psi(s'+s'')) \right) \right. \right. \\ \left. \left. \left(\frac{\underline{\mu}_{ba}^* \cdot \underline{u}}{\mu_{ba}^*} E_{+q}(t-s'-s''-s''') \exp i(q\varphi - q\psi(s'+s''+s''')) + \frac{\underline{\mu}_{ba}^* \cdot \underline{u}}{\mu_{ba}^*} E_{+q}^*(t-s'-s''-s''') \exp -i(q\varphi - q\psi(s'+s''+s''')) \right) \right. \right. \\ \left. \left. + \text{c.c.} \right] + \text{c.c.} \right\} \quad 33$$

This equation simplifies for no atomic motion or for large doppler broadening. These cases are considered separately.

A. No Atomic Motion

For no atomic motion, that is $\dot{\psi} = 0$, equation 33 may be reduced by the following sequence of operations: (a) Complete the integration over φ . (b) Write E_{+q} in the form introduced by equation 15b, integrate the resonant terms over s''' , s'' , and s' . Then the polarization may be written as

$$P_{+q}^{(3)} = i \frac{N \hbar^{-3}}{2\pi} (\lambda_a/\gamma_a - \lambda_b/\gamma_b) (1/\gamma_a + 1/\gamma_b) \beta \left(\frac{2\gamma_{ab}}{(\omega_{ab} - \omega_0)^2 + \gamma_{ab}^2} \right) \left[\frac{(AA^* + 2BB^*)}{i(\omega_{ab} - \omega_0) + \gamma_{ab}} A e^{-i\omega_0 t} + \frac{(BB^* + 2AA^*)}{i(\omega_{ab} - \omega_0) - \gamma_{ab}} B e^{+i\omega_0 t} \right] \quad 34$$

where β is given by

$$\beta = \int dA |\mu_{ba}^* u|^2 |\mu_{ba}^* u|^2 \quad 35$$

B. Large Doppler Motion

For large doppler motion equation 33 may be reduced by the following procedure: (a) Complete the φ integration. (b) Perform the $\dot{\varphi}$ integration,

note that the integrals are of the form

$$\int_0^\infty ds' ds'' G(s', s'') \exp\{-\frac{1}{4} D^2 (s'' - s')^2\} \simeq 2D^{-1} \pi^{\frac{1}{2}} \int_0^\infty ds' G(s'', s') \delta(s'' = s')$$

$$\text{or} \quad \int_0^\infty ds' ds'' G(s', s'') \exp\{-\frac{1}{4} D^2 (s'' + s')^2\} < |G(\infty)| \quad 4\pi D^{-2}$$

and that the dominant contribution is from integrals of the first type.

(c) Write E_{+q} in the form introduced in equation 15b, integrate over s' and s'' and omit all non-resonant terms. Then the polarization is

$$P_{+q}^{(3)} \simeq \frac{iN \hbar^{-3}}{2\pi^{\frac{1}{2}} D} \beta (\lambda_a/\gamma_a - \lambda_b/\gamma_b) (1/\gamma_a + 1/\gamma_b) \left[\frac{BB^*}{i(\omega_{ab} - \omega_0) + \gamma_{ab}} A e^{-i\omega_0 t} + \frac{AA^*}{i(\omega_{ab} - \omega_0) - \gamma_{ab}} B e^{+i\omega_0 t} + \frac{AA^*}{\gamma_{ab}} A e^{-i\omega_0 t} - \frac{BB^*}{\gamma_{ab}} B e^{+i\omega_0 t} \right] \quad 36$$

Equation 34 gives the third order contribution to the polarization for atoms at rest and equation 36 for atoms with large doppler motion. It is expected that all other cases may be found between these two extremes and that the polarization may be expressed as

$$\vec{E}_c^{-1} P_{+q} \simeq (C_1 + C_2 |A|^2 + C_3 |B|^2) A e^{-i \omega_0 t} + (C_1^* + C_3^* |A|^2 + C_2^* |B|^2) B e^{+i \omega_0 t} \quad (37)$$

For atoms at rest the C coefficients have the form

$$C_j = C_j' + i C_j'' = \text{const} \frac{(\omega_{ab} - \omega_0) - i \gamma_{ab}}{(\omega_{ab} - \omega_0)^2 + \gamma_{ab}^2} \quad (38)$$

and C_1, C_2, C_3 differ in the choice of the constant term ^{as} indicated by equation 30 and 34.

C_1 is given by equation 30 for the first order polarization and the frequency dependence is given by the doppler broadening function $Z(\omega_0 - \omega_{ab}, \gamma_{ab}, D)$. For large doppler broadening $C_1' \sim 0$ and C_1'' is of the doppler form

$$C_1'' \simeq \text{const} \exp -(\omega_{ab} - \omega_0)^2 / D^2 \quad (39)$$

C_2 and C_3 are complex constants which range between the values given by equation 34 for atoms at rest to those given by equation 36 for atoms with larger doppler motion. For large doppler motion $C_2' \simeq 0$, $C_2'' \simeq \gamma_{ab}^{-1}$ and C_3'' has the same frequency dependence as given by equation 38. In third order the saturation in the polarization of the ccw traveling wave is due to both the ccw and cw traveling waves. This is apparent in equation 34 and 36 in which both AA^* and BB^* are coefficients of $A e^{i \omega_0 t}$. For large doppler broadening C_2'' is almost frequency independent and C_3'' has the frequency response given by equation 38. This is apparent in equation 36 in which BB^* is the

coefficient of $A e^{-i\omega_0 t}$. Although this may seem surprising, it was recognized by Lamb¹³ in his paper and is to a large extent responsible for hole burning. The frequency dependence of the C_1 coefficient is comparable to the doppler width of the line while the frequency dependence of the C_3 coefficient is comparable to the natural width of the line as indicated by equation 38. Thus the gain for $\omega_0 = \omega_{ab}$ may be less than for $\omega_0 \neq \omega_{ab}$ as shown in Figure 4. The cause of the effect can be seen by examining the following array.

	s'''	s'	s''	$(t-s'-s''-s''')$	$(t-s'-s'')$	$(t-s')$	
(1)	$+i\omega_0 s'''$	$+i\omega_0 s'$	$0s''$	-	+	-	$(AA^*+2BB^*)Ae^{-i\omega_0 t}$
(2)	- "	+ "	"	+	-	-	"
(3)	- "	- "	"	+	-	+	$(BB^*+2AA^*)C^{+i\omega_0 t}$
(4)	+ "	- "	"	-	+	+	"

First only resonant terms are kept and this restricts the coefficients of $\exp(i\omega s)$ for s''' , s'' , and s' to the values shown. The remaining signs are for the sign of $\exp(i - -)$ in the product $E(t-s')E(t-s'-s'')E(t-s'-s''-s''')$ shown explicitly in equation 33. The use of the full array gives equation 34 for atoms at rest. For atoms in motion a rapidly varying phase term $\exp(\pm i q \dot{\psi} s)$ must be considered. The dominant terms which survive the average over the random phase rate $\dot{\psi}$ are those for which $s''' = s'$ and the 12 terms are reduced to 4. The ^{frequency sensitive} coefficient of $Ae^{-i\omega_0 t}$ is given by one of the BB^* terms of in row 1. Thus the first interaction with

the field at $(t-s'-s''-s''')$ occurs with the B^* coefficient of the c.w. wave, the second interaction at $(t-s'-s'')$ with the B coefficient of the c.w. wave, and the interaction at $(t-s')$ with the A coefficient of the c.c.w. wave. The phase of this term is $\exp i q \dot{\varphi}(s'''-s')$, and for $s''' = s'$ survives the average over the random phase $\dot{\varphi}$; similar argument may be made for the AA^*A term.

OSCILLATIONS FOR THE ALMOST DEGENERATE MODE

Ideal System

Equation 14 for the equation of motion of the field and equation 37 for the polarization of the optical maser medium may be used for the discussion of the ideal system. For this purpose it is convenient to use the following notation.

$$A(t) = U e^{iu} \quad ; \quad B(t) = V e^{iv} \quad (40)$$

$$C_1 = C_1' + iC_1'' \quad ; \quad C_2 = C_2' + iC_2'' \quad ; \quad C_3 = C_3' + iC_3''$$

The frequency dependence of the C 's is given by equations 34, 36, 38 and 39. If terms of the type U and u are regarded as small, and $\exp +i(u - \omega_0 t)$, is assumed almost orthogonal to $\exp i(v + \omega_0 t)$, then equation 14 and 37 may be written as

$$\dot{u} = \Omega q + \frac{1}{2} \omega_0 (C_1' + C_2' U^2 + C_3' V^2) \quad (41a)$$

$$\dot{v} = \Omega q - \frac{1}{2} \omega_0 (C_1' + C_3' U^2 + C_2' V^2) \quad (41b)$$

$$2\dot{U} = - \omega_0 (Q^{-1} + C_1'' + C_2'' U^2 + C_3'' V^2) U \quad (41c)$$

$$2\dot{V} = - \omega_0 (Q^{-1} + C_1'' + C_3'' U^2 + C_2'' V^2) V \quad (41d)$$

A steady state constant amplitude requires $\dot{U} = 0 = \dot{V}$ and an obvious solution for the amplitude is

$$U^2 = V^2 = -(Q^{-1} + C_1'') / (C_2'' + C_3'') \quad (42a)$$

The two frequencies of oscillation are $\omega_{ccw} = \omega_0 - \dot{u}$ and $\omega_0 + \dot{v} = \omega_{cw}$ and the beat frequency is

$$\Delta\omega = \omega_{cw} - \omega_{ccw} = \dot{u} + \dot{v} = 2\Omega q \quad (42b)$$

To this degree of approximation the c.w. and c.c.w. modes are equally excited, the frequency of each mode is shifted an equal amount in the same direction by the frequency sensitive C' terms and the amplitude terms. The difference in frequency between the two modes is $2\Omega q$ and is not sensitive to the effects of saturation for the ideal system.

Equation 42a gives the stored energy energy, and the power output of each mode is

$$P_{cw} = P_{ccw} = \omega W / Q = \omega \epsilon_0 U^2 / Q = -\epsilon_0 (\omega / Q) (Q^{-1} + C_1'') / (C_2'' + C_3'') \quad (44)$$

For extreme doppler motion C_1'' has the doppler frequency response given by equation 39 and for $(Q^{-1} + C_1'') < 0$ the system oscillates. C_3'' has the response given by equation 38 and the frequency response of the power output is of the form

$$\left(-Q^{-1} + \text{const } e^{-(\omega_{ab} - \omega_0)^2 / D^2} \right) \frac{[(\omega_{ab} - \omega_0)^2 + \gamma_{ab}^2] \gamma_{ab}}{[(\omega_{ab} - \omega_0)^2 + 2\gamma_{ab}^2]} \quad (45)$$

and shows the dip in power output discussed by Lamb¹³. A typical power output curve is shown in Figure 4. "Frequency pulling" occurs as shown by equation 43 and for $\Omega = 0$

$$(\omega_{cw} - \omega_0) / \omega_0 = \frac{1}{2}(C_2' + C_3')V^2 \quad (46a)$$

where ω_{cw} is the frequency of oscillation for the p.c.w traveling wave and ω_0 the center frequency of the cavity. $(Q^{-1} + C_1'')$ is the linear gain of the oscillator. This is in agreement with the expression introduced by Townes¹⁴ when $(Q^{-1} + C_1'') \sim Q^{-1} = \Delta\omega_L / \omega$ and $2 \gamma_{ab} = \Delta\omega_{ab}$

$$\gamma \approx \gamma_0 + (\gamma_0 - \gamma_{ab}) \Delta\gamma_L / \Delta\gamma_{ab} \quad (46b)$$

Equation 42a gives the obvious and desirable solution to the problem. The stability of the solution is now examined. In order to simplify the discussion of the problem the following notation is introduced,

$$X = U^2 \quad Y = V^2 \quad (47a)$$

$$h = -\omega_0(Q^{-1} + C_1'') \quad g = -C_2''(Q^{-1} + C_1'')^{-1} \quad f = -C_3''(Q^{-1} + C_1'')^{-1} \quad (47b)$$

and equation 41c and 41d may be written as

$$\dot{X} = h(1 - gX - fY)X \quad (41c')$$

$$\dot{Y} = h(1 - fX - gY)Y \quad (41d')$$

Stable solutions with $\dot{X} = 0 = \dot{Y}$ are desired. Following the standard procedure¹⁵ in phase trajectories the equation

$$\frac{dY}{dX} = \frac{(1 - fX - gY)Y}{(1 - gX - fY)X} = \frac{P(X,Y)}{Q(X,Y)} \quad (48)$$

is examined. The singularities of interest occur at $P = 0 = Q$. The singularities are shown in Figure 5 and occur at $(X = 0, Y = 0)$,

$(X = 0, Y = 1/g), (X = 1/g, Y = 0)$ and $(X = Y = (g+f)^{-1})$. This latter singularity is of primary interest. The lines $(1-fX-gY = 0)$ and $(1-gX-fY = 0)$ are shown in Figure 5a and 5b and the path of the phase trajectory is horizontal as it crosses the one line and vertical as it crosses the other. The phase trajectories may be sketched as shown in Figure 5 or the stability may be examined near $(g+f)^{-1} = X_0 = Y_0$ by expanding about the singularity with the substitution $X = X_0 + x$ and $Y = Y_0 + y$. Either technique indicates that the singularity is stable if $f < g$ and unstable if $f > g$.

From this discussion it is apparent that stable oscillation at two frequencies ω_{cw} and ω_{ccw} requires

$$C_2'' > C_3'' \quad (48b)$$

This occurs for large doppler broadening. For atoms at rest $C_2'' < C_3''$ and oscillations at two frequencies is not stable. Even for large doppler broadening C_3'' is frequency sensitive and as the cavity frequency ν_0 is tuned near ν_{ab} , $C_3'' \simeq C_2''$ and the two lines coincide and this is very near an unstable point for the system.

In this ideal case and for large doppler broadening, $C_2'' > C_3''$ and $U^2 = V^2$ is a stable singular point and stable oscillations at the two frequencies ν_{cw} and ν_{ccw} occur. Equations 42a and 42b are appropriate. Beats due to rotation are expected as the cavity frequency ν_0 is tuned over the entire doppler width. Only near $\nu_0 \simeq \nu_{ab}$ does the system approach an unstable point.

Bias Beats

Equation 14 is now extended to include an external source which couples into the cavity through a unidirectional coupler. Figure 5 shows a unidirectional coupler which feeds the energy of the c.c.w. mode into the c.w. mode, but not in the opposite sense. Equation 14 may be written as

$$\ddot{E}_{+q} + \omega_0^2 E_{+q} - i2\Omega_q \dot{E}_{+q} = \omega_0^2 \epsilon_0^{-1} \frac{P_q}{Q} \frac{\omega_0}{Q} \dot{E}_{+q} + \frac{i\omega_0^2}{Q_B} A e^{+i\omega_0 t} \quad (49)$$

Q_B is a measure of the coupling or power transferred and is regarded as small compared to Q in this calculation. Equation 40a, 40b, 40c remain unchanged for real Q_B and 40d is modified to read

$$2\dot{V} = -\omega_0(Q^{-1} + C_1'' + C_3''U^2 + C_2''V^2)V + \omega_0 Q_B^{-1} U \quad (50)$$

Steady state conditions require $\dot{U} = \dot{V} = 0$. U^2 and V^2 are related by

$$U^2 - V^2 = (Q_B(C_3'' - C_2''))^{-1} U/V \quad (51)$$

and the beat frequency between the two waves is

$$\omega_{cw} - \omega_{ccw} = \dot{u} + \dot{v} = 2\Omega_q + \Delta\omega_{bias} \quad (51a)$$

$$\Delta\omega_{bias} = \frac{1}{2} \omega_0 (C_2' - C_3')(U^2 - V^2) \quad (51b)$$

For small coupling, $Q_B \gg Q$, the shift in U is small and $U/V \simeq 1$, and the bias beats are approximately given from equations 51a and 51c by

$$\Delta\omega_{\text{bias}} \simeq \frac{1}{2} \omega_0 (C'_2 - C'_3) / (C''_2 - C''_3) Q_B \sim \frac{1}{2} \omega_0 (\omega_{\text{ab}} - \omega_0) Q_B \sqrt{\frac{1}{\omega_{\text{ab}}}} \quad (51c)$$

This equation is only valid for the cavity frequency ν_0 well away from the atomic frequency ν_{ab} , but does indicate that the bias decreases as the cavity is tuned away from the atomic frequency. Mr. Little, a graduate student in our laboratory, has observed this effect as the cavity is tuned through the atomic frequency ν_{ab} .

In order to examine this problem in some detail the notation introduced by equations 47a and 47b and 41c' and 41d' is used. The equations of interest may be written as

$$\dot{X} = h(1 - gX - fY)X = Q(X, Y) \quad (52a)$$

$$\dot{Y} = h(1 - fX - gY)Y + m(XY)^{\frac{1}{2}} = P(X, Y) \quad (52b)$$

and

$$\frac{dY}{dX} = \frac{h(1 - fX - gY)Y + m(XY)^{\frac{1}{2}}}{h(1 - gX - fY)X} = \frac{P(X, Y)}{Q(X, Y)}$$

is the slope of the phase trajectory.

$$m = \omega_0 / Q_B \quad n = \omega_0 / Q_A \quad (52c)$$

Some of the singularities are shown in Figure 6a. Again the singularity near $X = Y$ or $U^2 = V^2$ is of primary interest. The effect of the coupling term is to change the point of intersection such that $U^2 - V^2 \neq 0$, and as indicated by equation 51b a bias beat frequency is observed in the absence of rotation. The system is more sensitive to tuning the

cavity near the atomic frequency ν_{ab} , and it is apparent from Figure 6b that the two lines may no longer intersect at any point. Thus as the cavity is tuned from a frequency lower than ν_{ab} or higher than ν_{ab} Figure 6a applies and bias beats are given by equation 51d. As ν_0 approaches ν_{ab} , Figure 6b is more appropriate and a stable singularity does not occur. The position of the singularity is quite dependent on Q_B or the coupled power. As m/h increases the two singularities rapidly approach each other. Q_B may be estimated from the coupled power $P_B = \eta P_L$,

$$Q_B = Q P_L / P_B = Q / \eta \quad (53)$$

where P_L is the power in the maser beam.

If power is scattered from each traveling wave into the other, then equation 41c is also modified and contains a term similar to equation 52a. The equations of interest are of the form,

$$\begin{aligned} \dot{X} &= h(1-gX-fY)X + n(XY)^{\frac{1}{2}} = P(XY) \\ \dot{Y} &= h(1-fX-gY)Y + m(XY)^{\frac{1}{2}} = Q(XY) \end{aligned} \quad (54)$$

and the singularities formed by the intersections of the curves $P(X,Y) = 0$ and $Q(X,Y) = 0$ are of interest. Figure 7a, and 7b are sketches of cases which occur as the cavity frequency ν_0 is tuned through ν_{ab} . If the coupling is large intersection may not occur and stable oscillation at two frequencies is not possible.

The coupling between the cw and ccw traveling waves which is due to

scattering may be estimated in the following manner. Suppose the fraction of the power scattered is $P_B = \xi P_L$ or $P_A = \xi P_L$. In order to be effective the radiation must fall within the angular spread of the maser beam $\Delta \Omega \sim (\text{spot size})/4\pi L^2$. The spot size is of the order of $L\lambda$ and the coupling Q_B or Q_A may be estimated from

$$P_B/P_L = Q/Q_B \approx \xi \Delta \Omega \sim \xi \lambda / 4\pi L \quad (55)$$

For $\xi = 0.01$, $\lambda \sim 10^{-6}$ m, $L \sim 1$ a coupling Q_B of the order of $10^9 Q$ is expected. This may be used with equation 51c to estimate the bias.

Entrainment of Frequency

A large class of oscillator problems are of the form

$$\ddot{y} + \omega_0^2 y = ay - by^3 + \omega_0^2 Y \cos(\omega t + \phi) \quad (56)$$

where a is the linear gain term, by^2 the saturation term, and the final term on the left hand side the effect of an external source. This problem has been examined in detail by Andronow and Witt¹⁵. In the absence of the external source, self oscillation occurs for $a > 0$, and then $y(t) = A \cos(\omega_0 t - \phi)$. The amplitude of oscillation $A^2 = 4a/3\omega_0^2 b$. If the external source term is included the frequency of the oscillator is entrained or "locked" to the frequency of the source if

$$|\omega_0 - \omega| < \frac{1}{2} \left[(a\omega/Q)(P_e/P_L) \right]^{\frac{1}{2}} \quad (57a)$$

Since a is comparable or less than ω/Q , an estimate for entrainment can be made by making this substitution. Then the upper limit for the bandwidth for entrainment is approximately related to the cavity width by

$$(\Delta\nu)_{\text{locking}} < \Delta\nu_L (P_e/P_L)^{\frac{1}{2}} \quad (57b)$$

For $\Delta\nu_L \sim 10^6$ and $P_e/P_L \sim 10^{-6}$ locking is expected in the kilocycle range. Smaller coupling and operation at lower power levels, smaller

a , reduce the bandwidth for entrainment. If $a = -\omega(Q^{-1} + C_1)$ is used in equation 57a and then equation 44 is used, a more exact determination of the locking frequency can be made. An approximate alternate form of

57a is

$$|\omega_0 - \omega| < \frac{1}{2}(3bP_L P_S/P_L)^{\frac{1}{2}} \quad (58c)$$

and 3b is associated with $3b = \omega(C_3'' + C_2'')$

This analysis does not constitute a proof that entrainment occurs for the ideal oscillator, but does indicate that coupling between modes by external objects can introduce a condition similar to that for the entrainment of an oscillator by an external source. An estimate of (P_e/P_L) for the unidirectional effect permits an estimate of the frequency region in which a more exact analysis is needed.

EVALUATION OF THE OPTICAL MASER PHOTON RATE GYROSCOPE

Cavity Resonator Design

Some of the cavity designs which are being used for the photon rate gyroscope in the infra-red and in the optical maser spectral region are shown in Figure 1. Although four mirrors were used in the initial designs, the three mirror cavity has many advantages. Figure 8 shows the square Fabry-Perot resonator which was used by Cheo and which is now modified into a three mirror system by Little. In the plane of the oscillator the three mirror cavity has closure properties for the rays in this plane and the mirror adjustments for tuning are about 1/10 less sensitive than for the mirror adjustments perpendicular to the plane of the oscillator. Figure 9 shows a more symmetric three mirror system with a two mirror recombiner being used by Bupp in our laboratory. Cavities with all flat mirrors or with one curved mirror to reduce diffraction

losses are used. The mirrors may have either a metallic reflecting coating in the infra-red region or a multi-layer dielectric coating in the 0.5 to 1 micron spectral region. Internal reflecting prisms are being used rather than mirrors in some designs¹⁵.

The cavity is of course subject to external noise vibrations and thermal noise vibrations. The dominant effect on the shift in frequency is the change in peripheral length and $\Delta v/v \approx \Delta L/L$. The elastic energy associated with this deformation is $\frac{1}{2} E_Y V(\Delta L/L)^2$ and this is of the order of kT for thermal noise. Thus the cavity frequency is subject to noise fluctuations of the order of

$$(\overline{\Delta v^2})^{\frac{1}{2}} \approx v(2kT/E_Y V)^{\frac{1}{2}} \quad (59)$$

This is of the order of lcps for most materials and reasonable volumes, and does not introduce problems in the present designs. The individual mirror mounts must be reasonably rigid against displacement. In one design an angular adjustment of 10^{-4} radians is sufficient to tune through the region of bias beats ^{of about ± 20 Kc.} External noise may be considered as raising the thermal noise effect and can be considered by changing T to a higher effective temperature in equation 58. The various mirror mounts and mounting tables may have troublesome resonant frequencies, but these are not analysed here since each system is a special case.

If f is the fractional loss per pass around the path, then the cavity bandwidth or Q is

$$\Delta \nu_L = fc/2\pi L = \nu Q^{-1} \quad (59)$$

where L is the cavity length, $\Delta \nu_L$ the bandwidth of the cavity, and c the velocity of light. Since $f \sim 0.01$ and $L \sim 1$ meter for most designs, $\Delta \nu_L \sim 10^6$ for the cavities under consideration. Collins¹² has given a formula of the type

$$\nu_{mnq} = (c/L) \left[q + \frac{1}{2\pi} \left(n + \frac{1}{2} \right) \arccos \left(1 - \frac{L}{R} \cos \theta \right) + \frac{1}{2\pi} \left(m + \frac{1}{2} \right) \arccos \left(1 - L \cos \theta / R \right) + \frac{1}{2} \delta_{(n=\text{odd})} \right] \quad (60)$$

for the resonant frequency of a triangular mirror system similar to that shown in Figure 9. R is the radius of curvature of the curved mirror and L the path length. The frequency separation of adjacent modes of the same q and even or odd n is $c/2L$ and is of the order of 100 Mc for typical cavities. The transverse modes are separated by approximately 15 Mc for $\theta = 30^\circ$ and $L/R \sim 1$, and the mode separation is large compared to the cavity width.

Maser Media

The gain or maser media is now considered. The doppler width from equation 26b,

$$\Delta \nu_D = (D/\pi)(\ln 2)^{\frac{1}{2}} = 4.3 \times 10^9 / \lambda (\text{mass number})^{\frac{1}{2}} \quad (61)$$

where λ is in microns. Typical values are given in Table I. At the

line center, $\nu_0 = \nu_{ab}$, the linear gain term for a plane wave is related to C_1'' by

$$(\text{linear gain}) = 2\pi C_1'' / \lambda \quad (62)$$

and C_1'' is given by equation 30

$$\epsilon_0 C_1'' = N(\lambda_a/\gamma_a - \lambda_b/\gamma_b) \pi^{\frac{1}{2}} (1/3 |\mu_{ba}^{\nu}|^2) / \Delta D \quad (63)$$

With $N(\lambda_a/\gamma_a - \lambda_b/\gamma_b) = (N_2/\epsilon_2 - N_1/\epsilon_1)$ equation 62 may be placed in a form similar to that used by Faust and McFarlane¹⁷. They find for the lines of primary interest that the linear gain is

$$(\text{linear gain}) = 1.76 \times 10^{-17} S(\text{mass number})^{\frac{1}{2}} (N_2/\epsilon_2 - N_1/\epsilon_1) \quad (64)$$

more properly
 $/(a||\mu||b)|^2$

S is the line strength and appears to be related to the electric dipole matrix element by $|\mu_{ba}^{\nu}|^2 = S(e^2 a_0^2) = 0.72 \times 10^{-58} S$. Table I contains some typical values measured or used by Faust and McFarlane. For extreme doppler

Table I

Line	Linear Gain m^{-1}	$N(\lambda_a/\gamma_a - \lambda_b/\gamma_b)$	S	$\Delta \nu_D$	C_1''
Ne 1.152	0.12	1.5×10^{14}	10	8.3×10^8	2×10^{-8}
Ne 3.392	4	9 "	56	2.8 "	250 "
Ne 0.632	0.053	13 "	52	15 "	0.5
Xe 2.026	0.76	2.6 "	15	1.8 "	24 "
Xe 3.508	16	11 "	73	1.1 "	900 "

broadening the ratio of C_2''/C_1'' is given for $\gamma_0 = \gamma_{ab}$ by

$$C_2''/C_1'' \approx |\mu_{ba}|^2 / 3VA^2 \gamma^2 \sim 10^{-6} \text{ s} \quad (65)$$

γ is the decay rate of the energy levels and is related to the natural width by $2\gamma = \Delta\nu_n$. $\Delta\nu_n \approx 70 \text{ Mc}$ for the 1.15 micron Ne line¹⁸.

The matrix element and γ are interdependent and a simpler form for equation 65 should be possible.

The spectral purity of the maser oscillation is limited by spontaneous emission. The ultimate theoretical limit is given by¹⁴

$$\Delta\nu_{osc} \approx 8\pi h \gamma (\Delta\nu_L)^2 / P \quad (66)$$

Equation 66 yields at 1 micron

$$\Delta\nu_{osc} \approx 10^{-3} \text{ cps}$$

Javan, Ballik and Bond¹⁹ estimated the linewidth at 2 cps. Since the beats are between two modes in the same cavity, first order dimensional changes are not important, and this high spectral purity should permit the observation of beats of the order of this width. Mechanical vibrations are the most important limitation on the lower limit of the ideal system and this of course assumes that locking can be reduced in the ideal system to an arbitrarily small value.

Optimum Design Considerations

Stable oscillation at two frequencies occurs in the ideal system for $C_2'' > C_3''$ and therefore a maser medium with large doppler broadening is necessary. Since the non-linear problem posed by equations 40 has not been solved in detail, it cannot be stated with certainty that for frequency separation below a certain level that entrainment will occur between the ccw and cw modes and that oscillation occurs at a single frequency. If frequency entrainment occurs due to unidirectional coupling of the power of one beam into the other the phenomena of bias beats occurs and a problem similar to the entrainment of an oscillator by an external source occurs. Equation 57c suggests that the bandwidth for entrainment may be reduced by selecting a small value for the $(C_2'' + C_3'')$ coefficient and a low level for the oscillator power. The cavity Q should be as large as possible or the reflecting properties of the mirrors of the best quality. Furthermore any properties of the mirrors, Brewster angle windows, or other objects in the maser beam path which cause unidirectional coupling of power should be minimized. In order to avoid objects in the path the design shown in Figure 9 does not have Brewster angle windows, etc., but is entirely enclosed. The maser beam path is free from foreign objects, dust, moisture, etc. and the only surfaces are the mirrors.

Some recent research by Little indicates that even the maser tube may be effective. In the apparatus shown in Figure 8 and operating at

3.39 microns, it was found that the insertion of an ordinary quartz tube in the beam path enhanced the power level of oscillation. The increase was proportional to the tube length. This was interpreted as small angle reflection, and for these very small angles the interior walls of the tube form very high quality surfaces. Further research by Little indicated that pyrex gave the largest effect and inconel metal tubes were comparable with quartz. For tubes 4.5 mm in diameter the power level of oscillation was attenuated, at 6 mm the power level could be increased by a factor of 3 with sufficient length of tubing, and at 7.5 mm the effect of the tube was negligible on the power level of oscillation. A 6 mm tube with a rough internal surface reduced the signal.

EXPERIMENTAL APPARATUS

A series of slides will be shown of the experimental apparatus. Tuning procedures, apparatus construction, and overall operation will be discussed with these slides.

References

* This work supported in part by NASA Grant No. NsG-552

1. A. A. Michelson, Phil. Mag. 8 716 (1904)
2. G. Saynac, Compt. Rend. 157 708 and 1410 (1913); F. Harress, dissertation, Jena, 1911 (unpublished); and B. Pogany, Ann. Physik 85 244 (1928)
3. A. A. Michelson and H. G. Gale, J. Astrophys. 61 1401 (1925)
4. C. V. Heer, Bull. Am. Phys. Soc. 6 58 (1961)
5. C. V. Heer, "Proceedings of the Third International Conference on Quantum Electronics" (Dunod Cie, Paris, and Columbia University Press, New York 1963) p 1305
6. C. V. Heer, Phys. Rev. 134 799 (1964)
7. C. V. Heer - proposal submitted to NASA, AFOSR, and ONR on 16 March 1961
C. V. Heer - Annual progress report to NSF - 6 January 1960
8. C. V. Heer - supplementary material supplied upon request to NASA 29 January 1962 and copies to AFOSR and ONR
9. W. Macek and D. Davis, Appl. Phys. Letters 2 (1963)
10. P. K. Cheo - Ph.D. dissertation, Ohio State University 1964;
P. K. Cheo and C. V. Heer, Applied Optics 3 788 (1964)
11. A. G. Fox and Tingye Li, Bell System Tech. J. 40, 453 (1961)
12. S. A. Collins, Jr. - Applied Optics - (to be published);
G. D. Boyd and J. P. Gordon, B.S.T.J. 40 489 (1961), 41 1347 (1962);
A. G. Fox and T. Li, Proc. I.E.E.E. 51 80 (1963); P. O. Clark,
Proc. I.E.E.E. 51 70 (149) (1963).
13. W. E. Lamb, Jr. Phys. Rev. 134 1429 (1964)
14. C. H. Townes, "Advances in Quantum Electronics," (Columbia University Press, New York, 1961) p3
15. A. Andronow and A. Witt, Archiv für Elektrotechnik, 24 (1930);
N. Minorsky, "Non-Linear Mechanics", (J. W. Edwards, Ann Arbor, 1947, p. 341)
16. J. E. Killpatrick (private communication)
17. W. F. Faust and R. A. McFarlane, J. Appl. Phys. 7 2010 (1964)
18. W. R. Bennett, Jr. Phys. Rev. 126 580 (1962)
19. A. Javan, E. A. Ballik, and W. L. Bond, J. Am. Opt. Soc. 52 96 (1962).

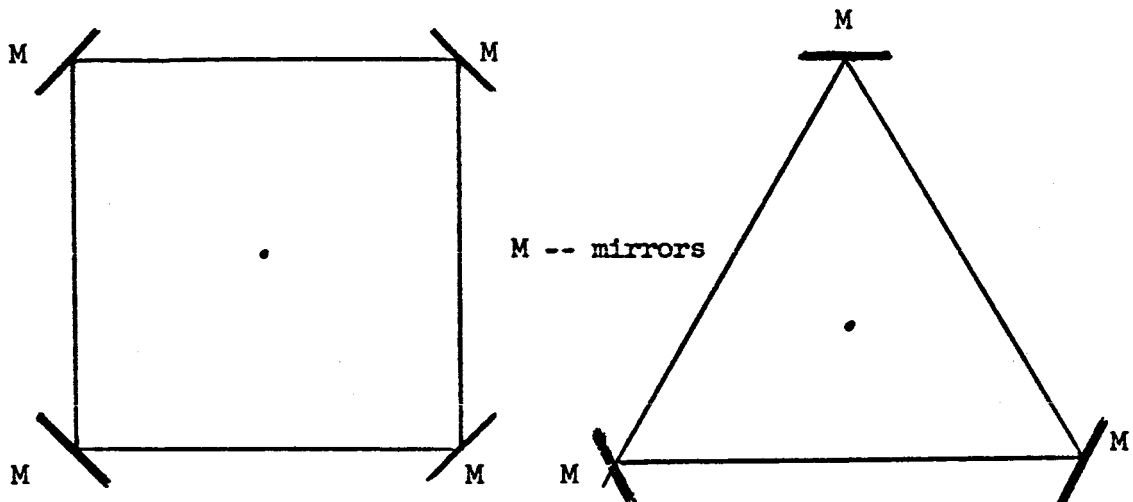


Figure 1
Typical Cavity Designs

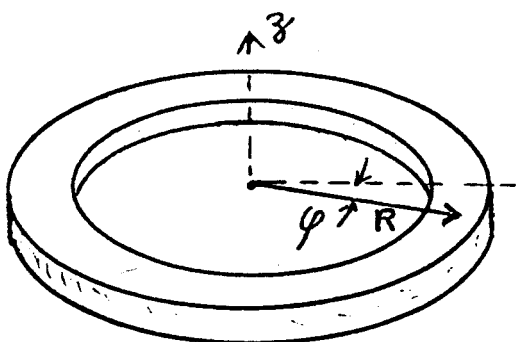


Figure 2
Ideal Cavity

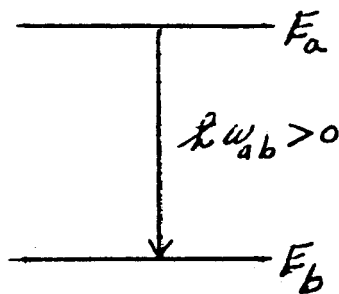


Figure 3
Energy Levels

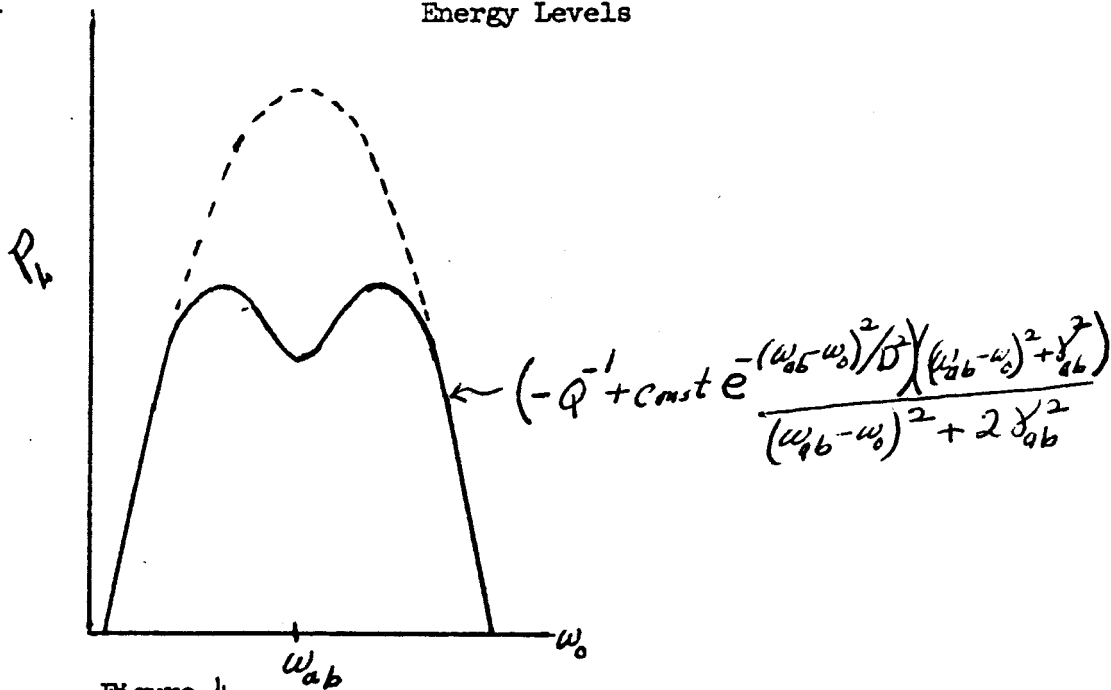


Figure 4
Power Dip at ω_{ab} by Tuning

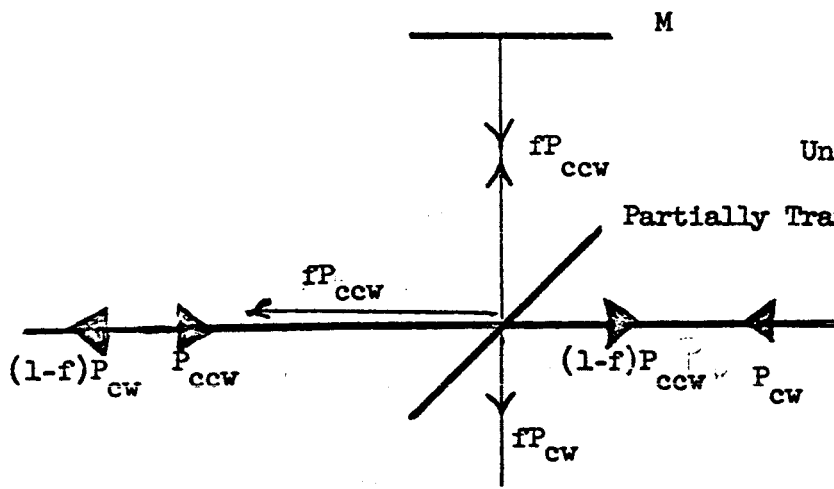


Figure 5
Unidirectional Coupler

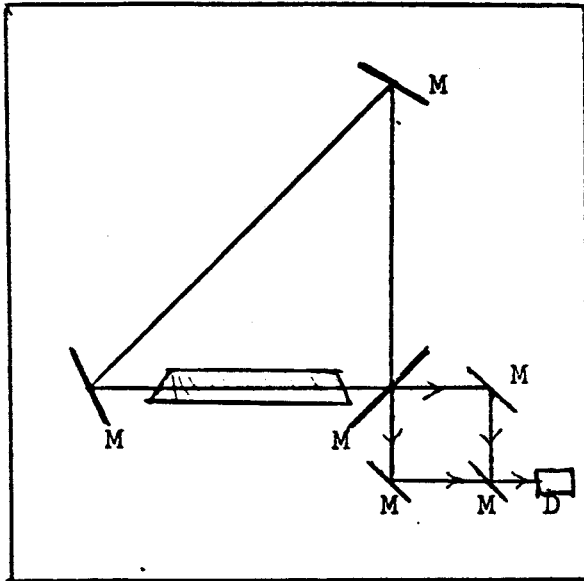


Figure 9
Photon Rate Gyroscope

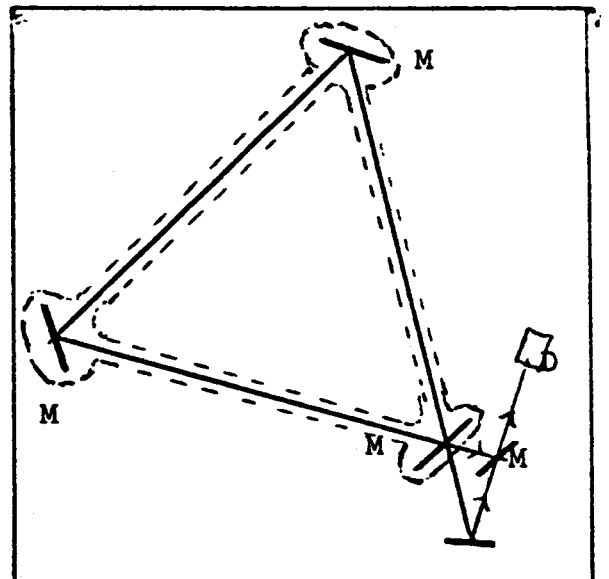


Figure 8
Photon Rate Gyroscope

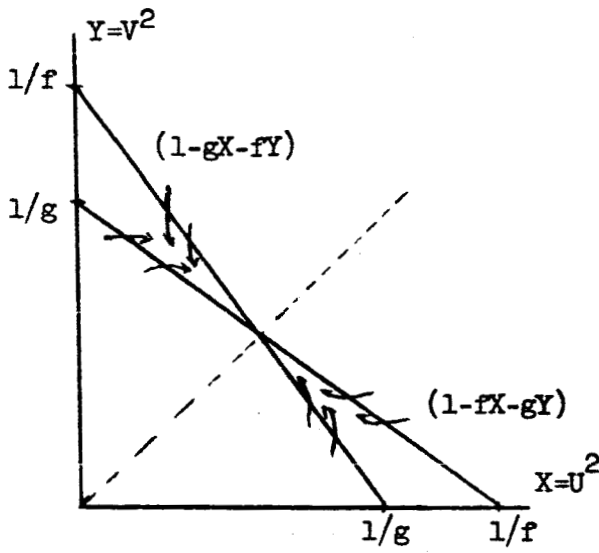


Figure 5
(See equation 48)

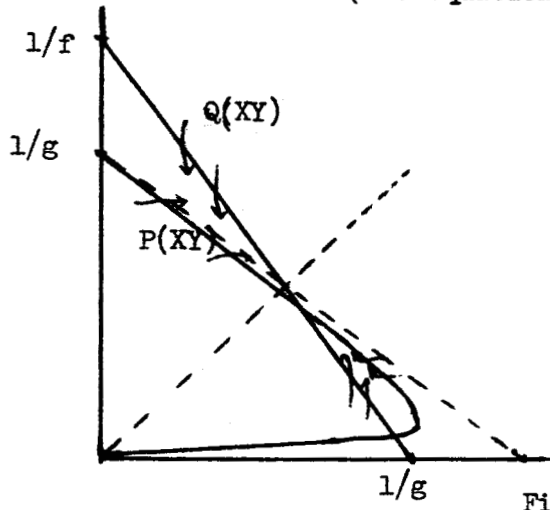
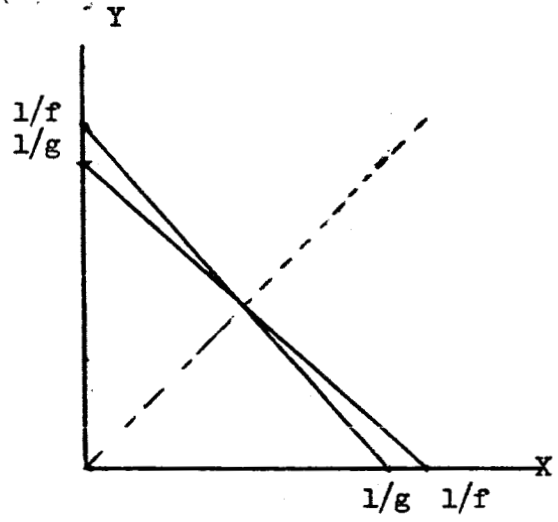


Figure 6
(see equation 52)

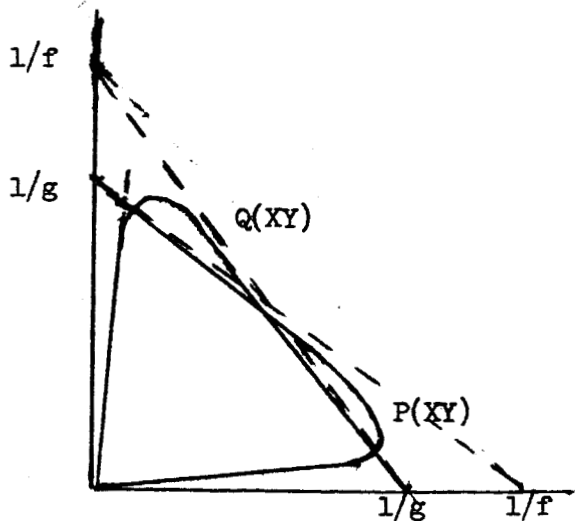


Figure 7
(see equation 54)